Development and Demonstration of Bi-directional Battery Charger for E-Mobility Charging Station

Hyunjun Choi[1], Sun-pil Kim[2], Jung-hoon Ahn[1], Dong-Hwan Park[1] and Sung-geun Song[1]

[1] Korea Electronics Technology Institute (KETI)

[2] GNEPS CO., Ltd

***Abstract*-- In this paper, a modular system was designed to connect E- mobility such as electric motorcycles to the battery charging station. The proposed modular system consists of an AC-DC converter and DC-DC converters. For AC-DC converters, although the grid-connected inverter is used prevalently, it has a large filter under a low switching frequency. A bridgeless totem-pole-based power factor correction (BT-PFC) is applied for high efficiency and high-power density. The 3-kW BT-PFC is implemented to handle the two battery packs. In the case of CC-CV chargers can be used in consideration of the battery charging characteristics. Since the nominal voltage of the Li-ion battery is about 36V, an isolated DC-DC converter is applied for voltage step-down from 400V to 50V. Also, the bi-directional buck-boost converter is connected in series to control the battery voltage. Experimental results with a 3.3-kW laboratory prototype battery charger validate the effectiveness of the proposed development.**

***Index Terms*—Modular converter, battery station, battery charger, E-mobility.**

I. INTRODUCTION

Recently, the need for green energy is rapidly increasing in new southern countries such as Vietnam to reduce air pollution. For example, Vietnam has the second-highest motorcycle ownership in the world. Several and high- density of gasoline-powered personal motorcycle has pressured traffic infrastructure and this is one of the critical reasons to air pollution. For this reason, the government is actively pushing for a policy to replace gasoline motorcycles with E-mobility, an electric two-wheeled vehicle. Due to reasonable purchase prices and low operating costs, E-mobility such as e-bikes and electric motorcycles can be a promising solution to replace gasoline-powered motorcycles [1].

To facilitate this transition, it is necessary to implement support infrastructure such as the charging station. Even though the charging station is installed rapidly due to rapid urbanization and investment in the power sector, when it is connected to a weak power system, the reliability of the power system becomes problematic. A large-capacity ESS can solve this problem [2]. However, the recent ESS fire caused a problem of avoiding installation in buildings or residences. For that problem, research of acceptability and power system stabilization by using ESS functions using batteries of electric motorcycles is studied [3].

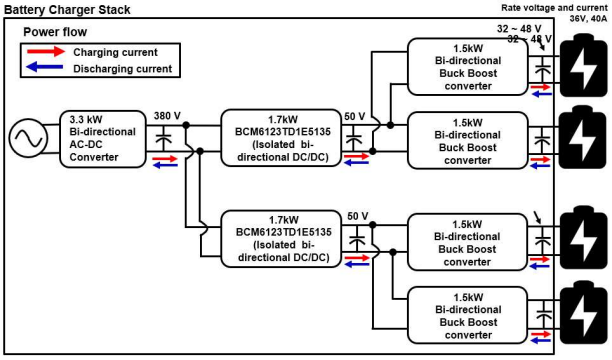

Fig. 1. Structure of battery charger

Fig. 1 shows the proposed bidirectional battery charger. It consists of three stages: a bi-directional AC-DC converter, an isolated bi-directional DC-DC converter, and a step-down DC-DC converter. The target of the AC-DC converter is 3.3 kW. The DC-DC parts are divided into 2 stages. First is the isolated converter with a high turn ratio. Second is the bi-directional buck/boost converter. For a high step-down converter is applied, which can converter voltage from 400 V to 50 V. Target of the isolated bi-directional DC-DC converter is 1.7 kW and it is connected in series to the AC-DC converter. In series, to control the output voltage connecting the battery, a bi-directional buck/boost converter is applied. Finally, the proposed battery charger performs four battery charging/ discharging simultaneously.

II. TOTEM-POLE BRIDGELESS POWER FACTOR COLLECTOR (PFC)

As shown in Fig. 2, there are various topologies for a bi-directional AC-DC converter. To improve the power conversion efficiency of the AC/DC converter and DC/DC converter, it is required to obtain high output voltage. To minimize the reactive power, a power factor correction (PFC) converter of the AC grid interface is required where the sinusoidal AC current with in-phase AC voltage makes the power factor maximized. Therefore, the boost-based

©2023 KIPE

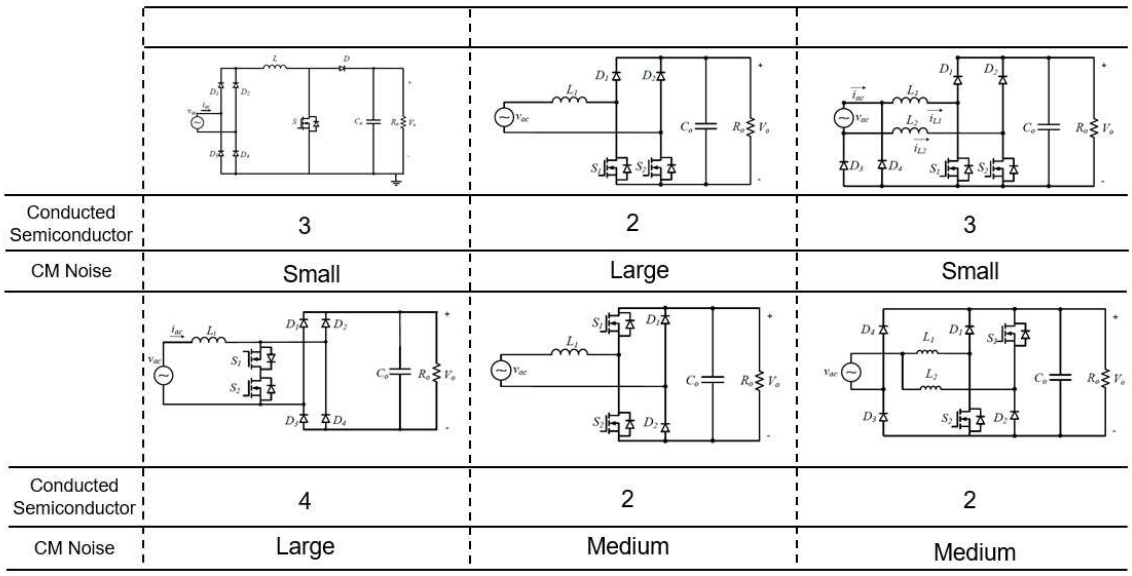

Fig. 2. Topologies for power factor collector [4], [5]

bi-directional AC/DC converter includes power factor correction (PFC). Compared with other topologies in Fig. 2, even though the totem-pole PFC has a medium level of CM noise, it has the least components and can reduce the number of semiconductor devices in the conduction path. Furthermore, by changing the Si-MOSFET to SiC MOSFET, it can solve the EMI issue from reverse recovery charge (*Qrr*), and achieve higher efficiency than before with low resistance and low capacitance [6]. In addition, the bi-directional capability can be obtained by replacing two low-frequency diodes with Si-MOSFET for the line rectification, which also takes advantage of low-condition losses.

A. Operation Mode

In the case of negative current of the conventional PFC converter, current flows through the body diode of the MOSFET. And that makes it difficult for bridgeless totem-pole PFC-based Si-MOSFETs to operate in CCM. In other words, the poor reverse recovery characteristics under the hard- switching conditions of the Si-MOSFET adversely affect the power conversion efficiency, resulting in high switching loss and high EMI emission. On the other side, trough the wide band gap devices such as GaN, SiC-MOSFET, higher efficiency can be achieved since the reverse recovery characteristic is much improved than conventional switches. Therefore, the either under the soft-switching and hard-switching, the power conversion efficiency can be improved to reduce the switching losses. In addition, under CCM operation, conduction losses from the inductor RMS current and EMI emission can be reduced since the peak of inductor current is reduced. Therefore, here, SiC- and Si-MOFSET are applied to the bridgeless totem-pole PFC (BT-PFC) converter as shown in Table I.

TABLE I
DESIGN SPECIFICATIONS OF TO TEMPLE -PFC CONVERTER

.	Quantity	Value
V_{ac_in}	AC input voltage	3.3-kW
V_{out}	Output voltage	176 V-265 V
P_{max}	Out max power	336 - 400 V
f_{sw}	Operating frequency	65 kHz
C_O	HVS filter capacitor	680 µF
S_1-S_4	MOSFET	IPW60R017C7
Q_1-Q_4	SiC MOSFET	IMZA65R046M1H
L	Inductance	420 µH
	Core/turns	CH400060

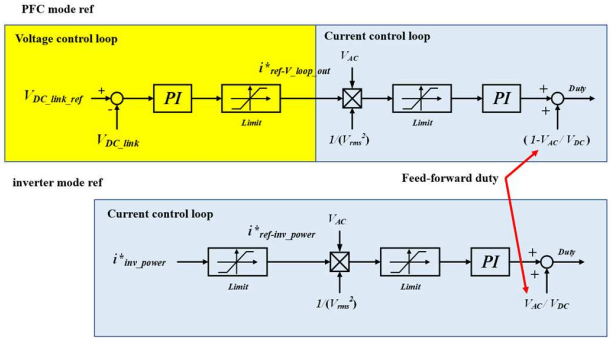

Fig. 3. Control block diagram

B. Parameter Design

One of the key components of BT-PFC under the CCM is the input inductor. Since under the CCM operation, inductance affects the current ripple, power density, and power conversion efficiency, the inductor design should consider the maximum peak input current. Since the value of inductance is in the trade-off between overall size and system efficiency, with consideration of the worst ripple case, inductance can be calculated with a 20% margin by using (1).

$$L = \frac{{V_O}^2 V_{in\_max} i_O}{1.7 V_{in} i_{in} P_O} \quad (1)$$

where P_O is the target output power V_{in} and I_{in} are the input voltage and input current, V_O and I_O are the output voltage and output current, and V_{in_max} is the maximum voltage when input is universal. As shown in Table I, under the specification, the inductor is designed as 420 μH by (1).

C. Power Control algorithm

Since the CCM operation can be implemented in BT-PFC with SiC MOSFET, average mode control can be used, which is most convenient method to control PFC [7] - [9]. As shown in Fig. 3, the controller is divided into PFC mode and Inverter mode, and only PFC mode, the current reference is generated. In PFC mode, the output voltage can be matched to refence voltage by using the voltage control. The output of voltage controller will be input of current controller to make inductor current as sinusoidal and in phase with input voltage by current control.

III. Bi-directional DC/DC Converter

In the case of the battery charger, since the input and output voltage are variable and depends on grid conditions and battery SoC, the power conversion efficiency of the bi-directional DC/DC converter is critical to the overall system efficiency.

A. Synchronous buck-boost converter with GaN-FET

Even though a non-isolated DC-DC converter does not use in commonly in high-power applications, it is usually used in battery applications due to advantages such as simple structure and simple control [10]. Especially, a synchronous buck-boost converter is usually used since this topology can achieve high-efficiency low-conduction loss based on low on-resistance and switching loss based on ZVS modulation. However, power loss in the synchronous buck-boost converter occurs due to the reverse recovery current of the parasitic internal diode. As explained in Section II, wide band gap power switch such as SiC-MOSFET and GaN has the advantage in terms of reverse recovery characteristic. Especially, since GaN can conduct current reverse bias without an internal diode, there is no reverse recovery current, and it can extremely reduce the switching losses. Therefore, as shown in Fig. 4, a GaN-FET-based synchronous buck/boost converter is selected to improve the power conversion efficiency and power density [11]

B. Parameter Design

The inductor design can be obtained as shown in (2).

$$L_s = \frac{V_O}{\Delta i_{Ls} f_{sw}}(1-D) \tag{2}$$

where L_S is inductance of buck-boost converter, D is duty ratio, Δi_{Ls} is the ripple ration of inductance current, and f_{SW} is switching frequency. This is very common method to design the converter. Here, there is two parameters to design the current ripple: inductance and switching frequency. As the inductance and switching frequency increase, the current ripple will be decreased. However, the higher the inductance, the lower the power density and the higher the switching frequency, the more sensitive it is to noise. Therefore, it is necessary to select an appropriate inductor and switching frequency in consideration of the trade-off relationship.

In the case of the output filter, most output voltage ripple is determined by the effective serial resistance (ESR), which is a parasitic component of the capacitor. In addition, the current passing through the capacitor is limited by the ESR. Therefore, so the ESR should be regarded as Equation (3) when design the output capacitance.

$$C_O = \frac{1}{8 f_{sw}\left\{\left(\frac{\Delta V_O f_{sw}}{V_O(1-D)}\right) - ESR\right\}} \tag{3}$$

TABLE II
Design Specifications of DC/DC converter

.	Quantity	Value
P_O	Output Power	1.5 kW
V_{bat}	Battery voltage (Li-ion)	30 V-42 V (36V / 40Ah)
V_{in}	Input voltage	42-50 V
I_{b_max}	Maximum battery current	40 A (1C)
L	Inductance	4.8 μH
D	Duty ratio	0.7-0.85
f_{sw}	Switching frequency	200 kHz
S_1-S_2	GaN FET	IPL60R075CFD7

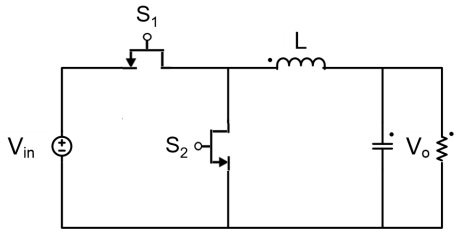

Fig. 4. Synchronous buck-boost converter with GaN-FET.

IV. Overall System Configuration of Proposed Battery Charger

Fig. 5 shows the overall structure of the proposed battery charger. A 3.3 kW converter module consists of a PFC converter and two DC-DC converters as explained in section II and section III. In detail, DC-DC parts consist of an isolated DC/DC converter and two synchronous DC/DC converters, each of which has a separate controller to perform charging/discharging control by controlling individual batteries which are master and slave modules. To cover the multiple E-mobility batteries and to increase the power capability of the charging station, the proposed modular systems are connected in parallel.

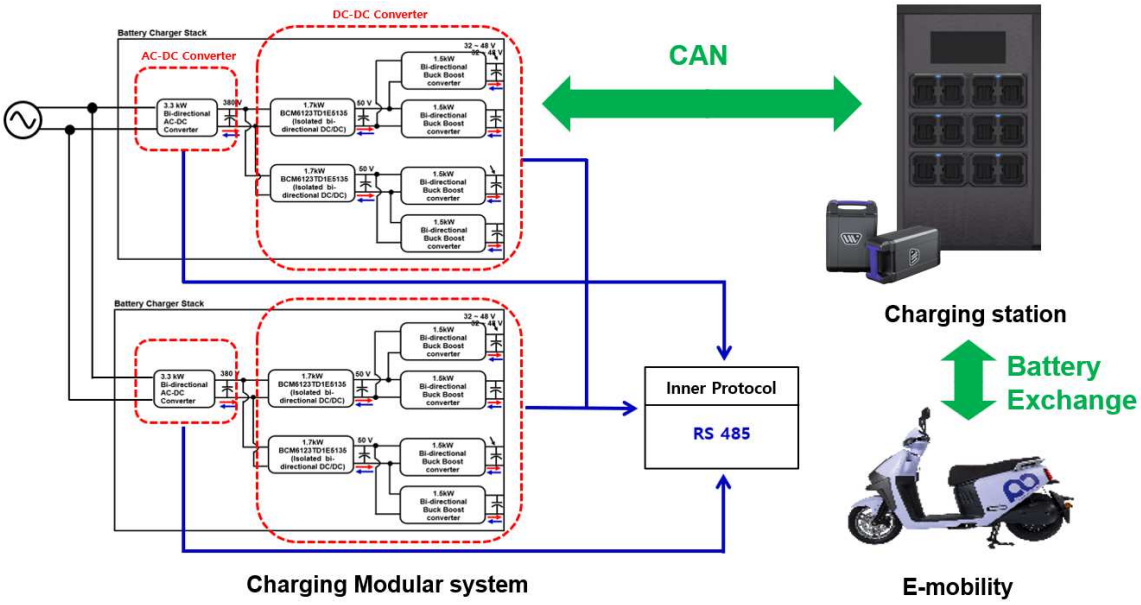

Fig. 5. Diagram of overall battery charger configuration with battery station.

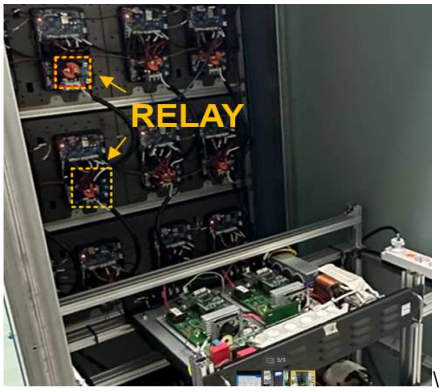

Fig. 6. Photograph of power station and battery charger interlocking test

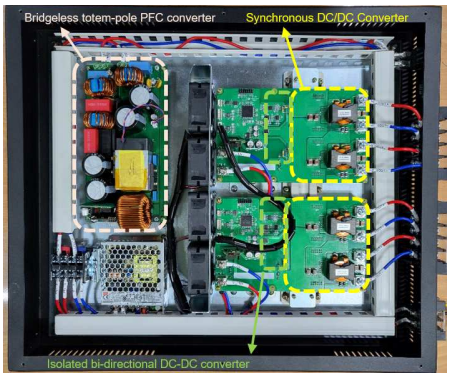

Fig. 7. Photography of modular battery charger.

As shown in Fig 5, the charging station has twelve battery slots. Even though the charging station can handle the multiple cells simultaneously, since the conditions of the new southern country, where is weak power system, the power is limited to 6.6 kW. It means that maximum charging/discharging current is limited to 0.5 C under the state steady operation. To cope with has multiple battery slots, as shown in Fig. 6, based on the system relay control according to the BMS information, it has designed a charging system structure that can charge multiple batteries in a circular manner. In DC-DC converter, master and sub module performs the communication with RS-485, and a BT-PFC is corresponding to master module of DC-DC converter based on the RS-485 and control the relay ON/OFF control. The internal DC/DC converter uses CAN to receive BMS information from the upper controller. That is, a 3.3kW modular system can transfer/transmit the information to/from upper controller by using CAN.

V. Experimental Results.

Fig. 7 shows the prototype of a modular battery charger. On the PCB of BT-PFC, to attenuate the noise, an EMI filter is deigned, and connected in series. Two parallel bi-directional DC/DC converter is connected with BT-PFC output and the isolated bi-directional DC/DC converters are inserted on the back of the PCB

A. Steady state operating waveforms

Fig. 8 shows the experimental results of the BT-PFC in battery charger under the 3 kW. The output is regulated as 398.5 V, the power factor is measured as 0.99, and efficiency is measured as 98.4%.

B. Interlocking Test

Fig. 9 shows the interlocking test between the battery charger and the 36V Li-ion battery. Fig. 9-(a) shows the battery current is controlled by the current command. The charge/discharge current of the battery was measured by changing the current command value from - 10A to 10A.

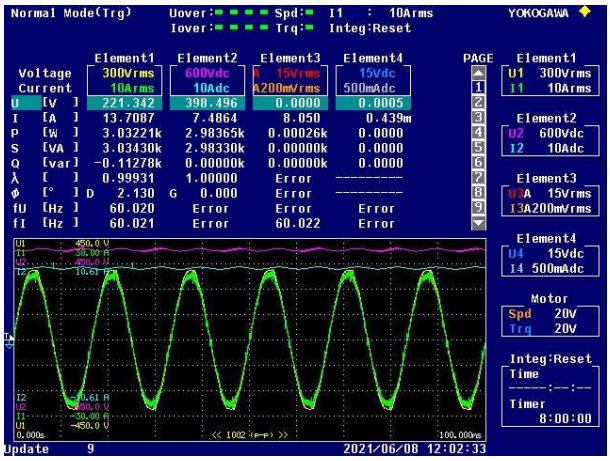

Fig. 8. Experimental results of bridgeless totem pole-PFC.

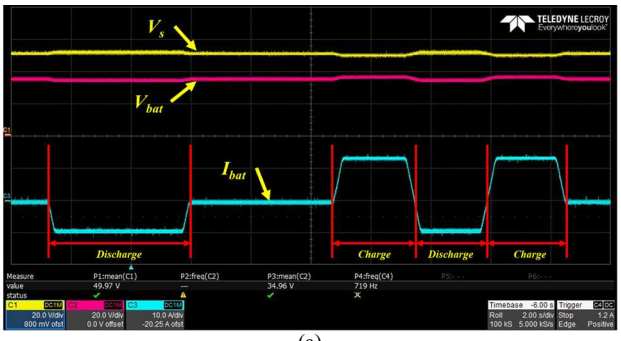

(a)

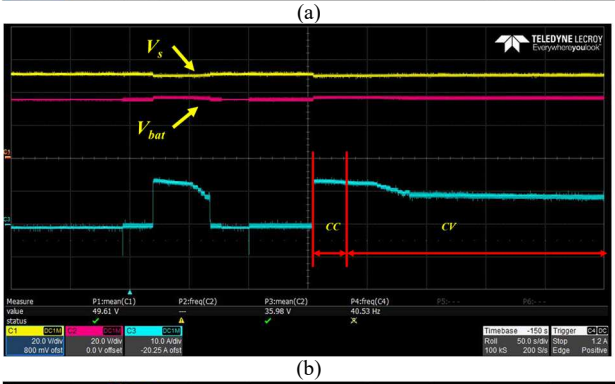

(b)

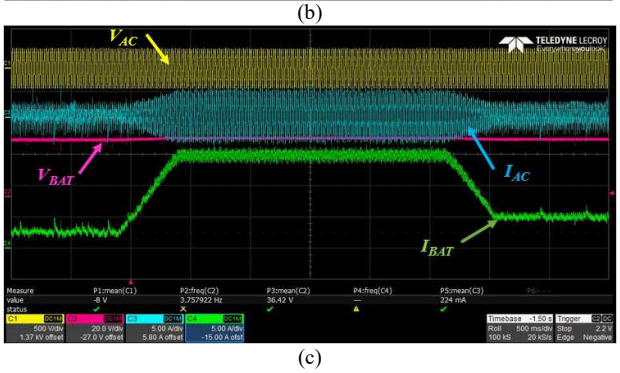

(c)

Fig. 9. Battery interlocking test: (a) CC-CV test with battery cell (b) charging/discharging current control test with Battery cell (c) charging /discharging current control test with Battery station

Here, it is confirmed that charging and discharging were carried out according to the command value. Fig. 9-(b) shows the CC-CV transition under the battery charging situation. Under the CC mode, the current is constant at 20 A (0.5 C), and when the CC-CV transition is started, the

(a)

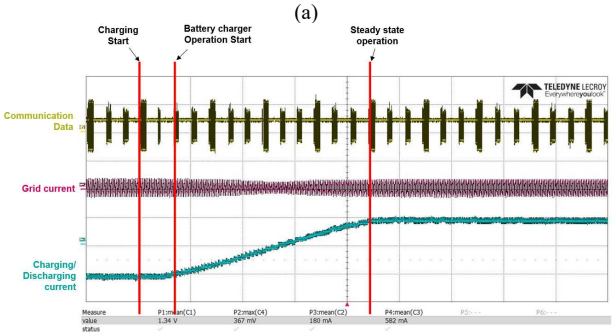

(b)

Fig. 10. Charging station interlocking test: (a) Battery charger Test-bed (interlocking with battery station) (b) Experimental results

magnitude of the current is smoothly reduced. To verify if the current value decreased according to the CV voltage control command value, the voltage control command value is changed and the corresponding current is changed. Fig. 9-(c) shows the experimental results under the grid-connected situation. The battery is charged by grid through the proposed battery charger with constant current, 20 A. Fig. 10. shows the interlocking test bed between a battery charger and a battery station with 12 batteries inserted. The communication. As shown in Fig. 10-(b), after receiving the charge-on command from EMS, the battery charger flows the current from the grid to the battery as 20 A.

VI. Conclusions

In this paper, the 3-stage converters for battery chargers are studied, developed, and demonstrated to interlock the battery station. In the case of the PFC converter, the WBG device-based BT-PFC is implemented. To increase the efficiency, and reduce the EMI noise, the CCM operation of BT-PFC is applied with simple control. In terms of the DC-DC converter, it was designed using the advantages of GaN-FET, which can conduct in the reverse direction with reverse recovery losses. Finally, the effectiveness of the proposed battery charger is verified by an interlocking test bed with a 6.6 kW battery charger where 12 batteries are inserted. The performance of the proposed battery charger is verified through the steady-state operation with the

battery station. At 850W, the highest efficiency of the battery charger system is measured as 95.1%.

ACKNOWLEDGMENT

This work was supported by the Korea Institute of Energy Technology Evaluation and Planning (KETEP) and the Ministry of Trade, Industry & Energy (MOTIE) of the Republic of Korea (No. 20208530050060)

REFERENCES

[1] D. N. Huu and V. N. Ngoc, ‘‘A research on the trend of transport electrification in Vietnam and the feasibility of PV-integrated charging station for electric two-wheelers at electric power university,’’ in Proc. 11th Int. Conf. Power, Energy Electr. Eng. (CPEEE), Feb. 2021, pp. 255–260.

[2] C. K. Lee and S. Y. R. Hui, “Reduction of energy storage requirements in future smart grid using electric springs,” IEEE Trans. Smart Grid, vol. 4, no. 3, pp. 1282–1288, Sep. 2013.

[3] Oceano, A.; Rodella, G.; Rizzo, R.; di Noia, L.P.; Brusaglino, G. Grid balancing support through Electric Vehicles mobile storage. In Proceedings of the 2020 International Symposium on Power Electronics, Electrical Drives, Automation and Motion (SPEEDAM), Sorrento, Italy, 24–26 June 2020; pp. 108–113

[4] Haoyi Ye, Zhihui Yang, Jingya Dai, Chao Yan, Xiaoni Xin and Jianping Ying, "Common mode noise modeling and analysis of dual boost PFC circuit," INTELEC 2004. 26th Annual International Telecommunications Energy Conference, Chicago, IL, USA, 2004, pp. 575-582.

[5] Q. Li, M. A. E. Andersen and O. C. Thomsen, "Research on Power Factor Correction boost inductor design optimization — Efficiency vs. power density," 8th International Conference on Power Electronics - ECCE Asia, Jeju, 2011, pp. 728-735,

[6] M. Pulvirenti, A. G. Sciacca, L. Salvo, M. Nania, G. Scelba, and G. Scarcella, “Body diode reverse recovery effects on SiC MOSFET half-bridge converters,” in IEEE ECCE, 2020, pp. 2871–2877

[7] B. Saglam, M. H. Aksit and B. Tamyurek, "A Comparison of GaN-Based Cascode and E-mode HEMTs Using Bridgeless Totem Pole PFC," 2022 IEEE Energy Conversion Congress and Exposition (ECCE), Detroit, MI, USA, 2022, pp. 1-6S

[8] B. Li et al., "GaN HEMT Driving Scheme of Totem-Pole Bridgeless PFC Converter," 2018 IEEE International Power Electronics and Application Conference and Exposition (PEAC), Shenzhen, China, 2018, pp. 1-6GaN

[9] T. T. Vu and E. Mickus, "99% Efficiency 3-Level Bridgeless Totem-pole PFC Implementation with Low-voltage Silicon at Low Cost," 2019 IEEE Applied Power Electronics Conference and Exposition (APEC), Anaheim, CA, USA, 2019, pp. 2077-2083

[10] Q. Cheng and H. Lee, "A high-frequency non-isolated ZVS synchronous buck-boost LED driver with fully-integrated dynamic dead-time controlled gate drive," 2018 IEEE Applied Power Electronics Conference and Exposition (APEC), San Antonio, TX, USA, 2018, pp. 419-422

[11] R. Elferich and C. Hattrup, "Minimum Loss Operation of the Synchronous Buck Converter Using Si, SiC, and GaN Transistors," PCIM Europe 2022; International Exhibition and Conference for Power Electronics, Intelligent Motion, Renewable Energy and Energy Management, Nuremberg, Germany, 2022, pp. 1-9.